Heavy Ion Beam Accumulation, Cooling, and Experiments at the ESR

B. Franzke, K. Beckert, F. Bosch, H. Eickhoff, B. Franczak, A. Gruber, O. Klepper, F. Nolden, P. Raabe, H. Reich, P. Spädtke, M. Steck, J. Struckmeier
GSI – Gesellschaft für Schwerionenforschung mbH
Postfach 110552, D-64220 Darmstadt, Germany

Abstract

The Experimental Storage Ring ESR — part of the heavy ion accelerator facilitiy at GSI — started operation early in 1990. This paper informs about the progress achieved in accumulation, electron cooling and internal experiments with fully stripped heavy ions from O^{8+} to U^{92+} at energies between 90 MeV/u and 300 MeV/u. Rf–stacking combined with compression in phase space by electron cooling turned out to be a very effective accumulation technique. Maximum numbers of stored ions for heaviest ions are determined by the equilibrium between accumulation rate and beam loss rate due to radiative electron capture of cooler electrons. Beam currents for lighter ions up to Ar^{18+} are limited by coherent instabilities. First excellent results of internal experiments with cooled, circulating beams of either primary ions or of secondary nuclear fragments confirm that the combination of the heavy ion facility Unilac–SIS–FRS with the storage ring ESR offers unique possibilities for atomic, nuclear and accelerator physics.

1 HEAVY ION FACILITY AT GSI

1.1 *The Unilac/SIS/FRS Complex*

The first stage of the accelerator facility at GSI, the Unilac, accelerates heavy ions up to Uranium to variable energies in the range 1.4 to 17 MeV/u. In 1992 a new high charge state injector combining an ECR source with RFQ and IH accelerating sections came in operation as an alternative to the old Wideröe pre–stripper section. Now the Unilac is able to supply low energy experiments and the injection line for the heavy ion synchrotron SIS [1] in a fast time sharing mode, based on the 50 Hz macro–structure of the beam, with different ions species and different specific energies. The 18 Tm–machine SIS extended in 1989 the range of available ion energies to 2 GeV/u for Ne^{10+} and to 1 GeV/u for U^{72+}–ions. Up to the present, the SIS has accelerated many different ion species from d^+ to U^{72+} to energies between 100 MeV/u and 2 GeV/u. Maximum intensities of 2×10^{10} light ions as O^{8+} and more than 1×10^7 heaviest ions as Bi^{67+} per accelerating cycle have been attained by radial stacking of up to 40 effective turns [2] at the injection energy of 11.4 MeV/u. Up to three users can be supplied by the SIS with beams of strongly different energy in a time sharing mode from cycle to cycle. Slow, resonant beam extraction with up to 10 s spill duration may alternate likewise with fast bunch ejection using the same extraction line. Fast ejection is used mainly to supply the ESR in the "double shot" mode, in which two of the four SIS–bunches are transferred by two steps to rf–buckets of the half–sized storage ring [2].

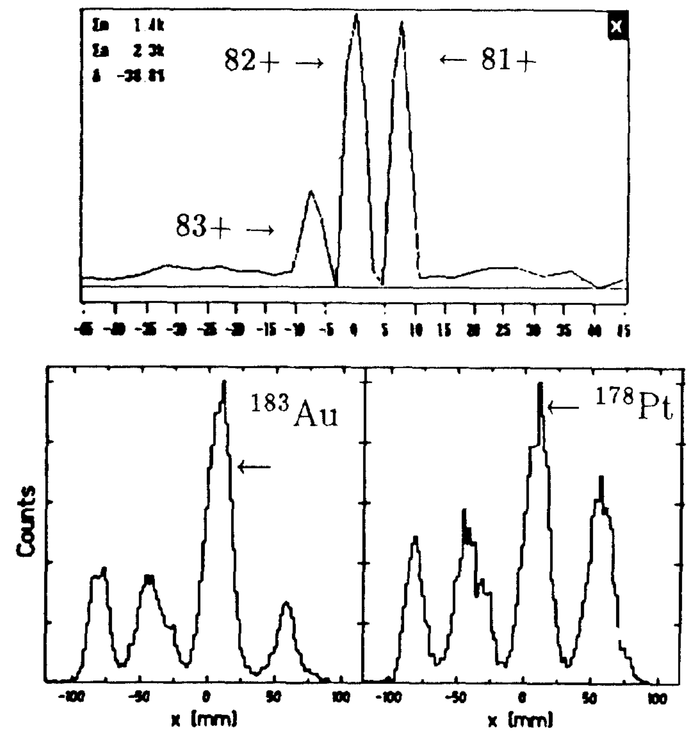

Figure 1: Typical distribution spectra after acceleration in SIS: for atomic charge states after one more stripping in 20 mg/cm^2 Cu of Bi^{67+} at 230 MeV/u (top) and for nuclear fragments of ^{197}Au at 950 MeV/u after a thick Al–target at different settings of the FRS.

Production of fully stripped ions with atomic numbers $Z \geq 36$ requires one more stripping in the transfer beam line. Alternatively, the transferred bunches may pass through a thick production target followed by the large FRragment Separator FRS [3]. By this way, separated beams of nuclear projectile fragments are delivered to ESR for injection, cooling and eventually accumulation. Examples for charge state distributions after the stripper and for nuclear fragment distributions after the production target and the FRS are displyed in fig. 1, beam transfer lines between the rings are shown in fig. 2.

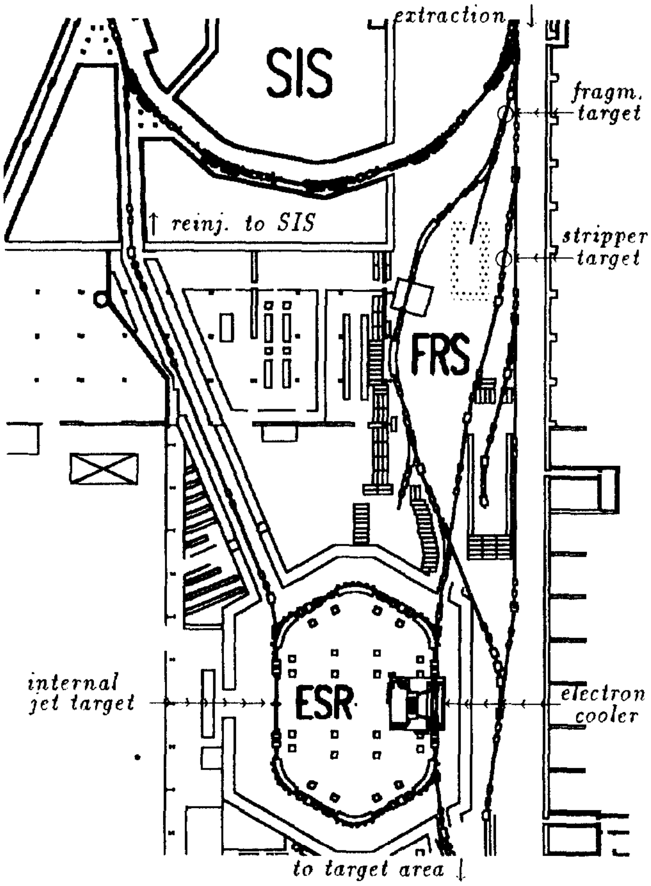

Figure 2: ESR with beam transfer lines from and to SIS.

1.2 *Experimental Storage Ring ESR*

The ESR design has been described in detail at past conferences [4], an impression of the ring structure is given in fig. 2. The following brief list may help to remind of most important ring features.

- The maximum bending power of 10 Tm allows storage of fully stripped ions at maximum energies between 560 MeV/u (U^{92+}) and 834 MeV/u (Ne^{10+}).
- Large acceptances in combination with flexible lattice optics are provided for beam accumulation, cooling of "hot" beams, storage of multi component beams, and, not least, for beam injection and extraction.
- Electron cooling (EC) at variable beam energies from 30 to 560 MeV/u serves for beam brillance as high as possible. It plays also an important role for beam accumulation and for internal experiments and facilitates the diagnosis of beam and lattice parameters.
- Special equipment is installed for investigations of interactions between cooled, circulating ions and internal gas jet atoms, free cooler electrons or laser beams.
- Acceleration or deceleration of cooled beams of fully stripped ions is in preparation for internal experiments at variable energy. Slow and fast extraction shall supply external experiments with highly brillant beams.
- Beam diagnosis applies mainly modern Schottky and beam transfer function (BTF) techniques. Active damping of coherent transverse beam oscillations has been practised already with some success. Emittances of circulating beams can be determined in a non destructive way using several movable position sensitive particle detectors, which deliver transverse distributions of ions after radiative electron capture (REC) in the cooler or in the internal gas jet.

2 APPLICATION OF ELECTRON COOLING

Recent results of electron beam cooling at the ESR are presented in a separate contribution to this conference [5]. the importance of the EC device [5] for ring operation and internal experiments may be deduced from following selection of examples.

2.1 *Beam Accumulation*

Beam accumulation in the ESR is done by combining the conventional rf-stacking method with electron cooling. The electron energy is suitably switched between injection and stack levels. At first, the injected bunches are compressed in order to avoid beam loss during deceleration to the stack. This is shown in fig. 3 by two longitudinal Schottky scans at different times after injection. The coasting stack

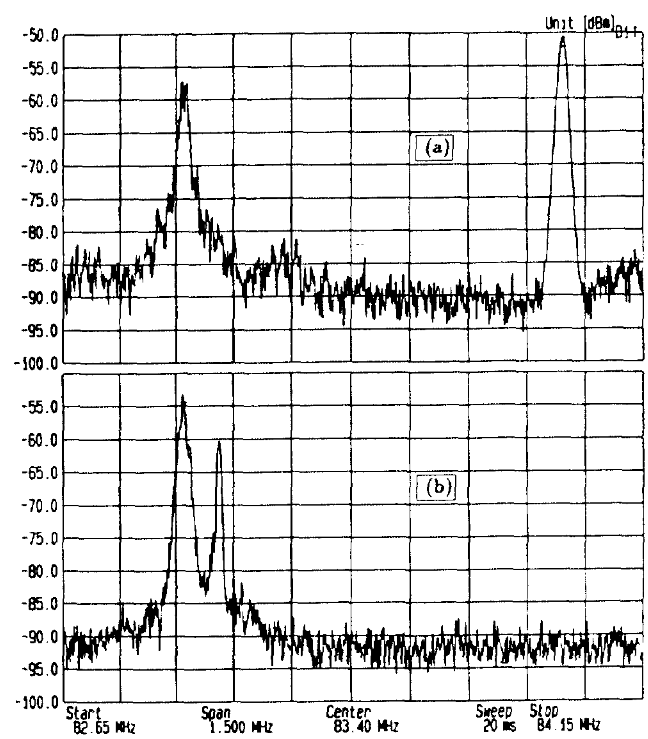

Figure 3: Combined Rf-stacking and electron cooling demonstrated by longitudinal Schottky scans at different times t after bunch injection: (a) $t = 2000$ ms: cooled bunches are still on injection orbit (right) and modulate the coasting stack (left) due to somewhat faster circulation. (b) $t = 2050$ ms: bunches are decelerated to the stack, while the rf amplitude is decreased already.

is cooled in the time between subsequent stacking processes. Since the phase space is "cleaned" all the time, beam accumulation is limited by other effects rather than by phase space. One of the principle beam current limits for this technique is determined by the equilibrium between the REC rate in the electron cooler and the accumulation rate. For high-Z, high-q ions the REC rate ($\propto q^2$) is high and the primary intensity is relatively low, mainly because of repeated stripping in the Unilac, before injection to and after acceleration in SIS. With Au^{79+} at 270 MeV/u, for instance, a saturation current of 1.4 mA, corresponding to 6×10^7 stored ions, was attained recently. The observed REC loss rate of about 5×10^{-4}/s is consistent with the injection of nearly 4×10^5 ions (10 μA) every 13 s. For cooled light ion beams ($Z \leq 30$), primary intensities are much higher and REC loss rates considerably lower. Up to now, the beam current is limited in this case to about 7 mA by coherent — mainly transverse — instabilities. Some success has been achieved already by an active feedback, the sources of high narrow band impedances in the frequency range 20 to 40 MHz, probably ferrite kickers, clearing electrodes with cables or the electrostatic septum, have to be found and deactivated in order to achieve essential beam current increase. For higher Z ions, the coherent oscillations seem to be damped more and more by intra beam scattering (IBS), which increases the equilibrium momentum spread in cooled beams approximately $\propto Z$ (see fig. 4). A list of ion species, energies and beam currents stored and cooled in the ESR is given in table 1.

Table 1: Ions, energies and beam currents in ESR by April 1993. The major part of beam currents I_i (number of ions N_i) has been recorded during physics experiments and may not be considered as upper limits.

Ion	Energy	N_i	I_i
$^{18}O^{8+}$	150 MeV/u	1.1×10^9	2.0 mA
$^{20}Ne^{10+}$	250 MeV/u	2.6×10^9	7.0 mA
$^{40}Ar^{18+}$	250 MeV/u	4×10^8	2.0 mA
$^{58}Ni^{28+}$	250 MeV/u	1×10^9	6.0 mA
$^{84}Kr^{36+}$	150 MeV/u	1×10^8	0.9 mA
$^{129}Xe^{54+}$	250 MeV/u	4×10^8	6.0 mA
$^{163}Dy^{66+}$	297 MeV/u	1×10^8	2.0 mA
$^{197}Au^{79+}$	270 MeV/u	6×10^7	1.4 mA
$^{209}Bi^{82+}$	230 MeV/u	5×10^7	1.2 mA
$^{238}U^{92+}$	300 MeV/u	2×10^7	0.6 mA

At energies above 90 MeV/u the life time of fully stripped or few-electron ions is determined only by REC in the cooler. With an EC current of 1 A the life time of Ne^{10+} beam at 150 MeV/u is nearly 7 hours. Though REC rates increase approximately $\propto q$, comfortable life times of about 1 h have been achieved also for U^{92+} and Au^{79+} beams by applying low EC current, e.g. 100 mA, without major reduction of the beam quality, even if ion beam currents are in the mA range. Beam loss due to residual gas interaction at pressures $\leq 10^{-10}$ mbar is negligible compared to that caused by REC in the cooler. A quite different situation is expected at low energies of about 10 MeV/u or with partially stripped ions ($Z - q \gg 1$). For example, strongly reduced life times of 300 s were observed with Bi^{67+} at 230 MeV/u and only 10 s with Ni^{15+} at 150 MeV/u, due to electron stripping at an average residual pressure of about 5×10^{-11} mbar. In experiments with the internal gas jet target the beam life is dominated by charge changing processes in the target itself. With an Ar-jet of 6×10^{12} atoms/cm^2 thickness a beam of fully stripped Dy^{66+} ions at 290 MeV/u lived only 150 s, mainly due to REC of bound target electrons.

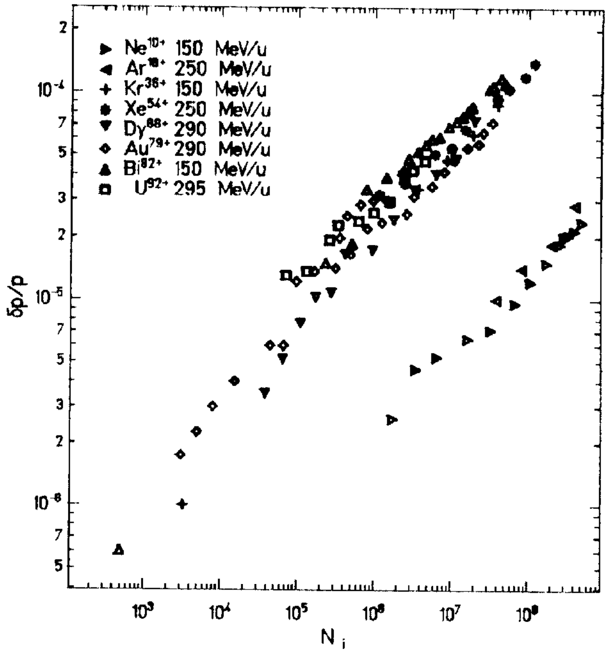

Figure 4: Equilibrium momentum spread $\delta p/p$ in electron cooled beams vs. number of stored ions N_i.

2.2 *Multi-Component Beam Storage*

The large momentum acceptance of the ESR and a special lattice optics with small dispersion on long straight sections makes it possible to store and cool simultaneously more than one charge state of an ion, e.g. two for Kr-, three for Au-, and even four for U-ions. The secondary charge states are populated by sequential REC in the cooler and are fixed to at nearly the same velocity by the cooler. Therefore, the relative frequency differences are determined only by orbit length differences $\Delta C/C$ due to charge differences $\Delta q/q$:

$$\frac{\Delta f}{f_q} = -\frac{\Delta C}{C_q} = \frac{1}{\gamma_t^2}\frac{\Delta q}{q} \tag{1}$$

Charge states q are known exactly and mean Schottky frequencies of cooled beams can be measured with high accuracy. Hence, the transition point for the given lattice optics, γ_t, can be derived with an accordingly high precision, typically in the order of 1×10^{-4}.

Other effects producing multi-component beams in the ESR itself are nuclear decay of stored primary nuclei and nuclear collisions in the internal gas jet target. There is also strong interest to inject and cool secondary beams of projectile fragments, aiming at precise mass determination for exotic nuclides. Electron cooling is the tool to reduce the momentum spread to extremely low values with a twofold profit. Both the spectral density in longitudinal Schottky spectra, i. e. the sensivity, and the precision of mass determination are enhanced essentially. A precise determination of γ_t is of comparable importance for planned mass measurements as are reproducibility and stability of both the magnetic bending field and the accelerating voltage of the electron cooler.

2.3 *Cooling of Radioactive Beams*

Injection and cooling of radioactive beams from the FRS was demonstrated with fragments of ^{20}Ne at 250 MeV/u by means of longitudinal Schottky spectra recorded immediately after injection and cooling to equilibrium. Besides the strong band from the primary ^{20}Ne, two weak bands from the isotonic fragments ^{18}F and ^{14}N were clearly separated in the spectrum, though the intensity fraction of fragments was only about 2×10^{-3}. As in the case of different ionic charge states, all nuclei are cooled to the same velocity. Using a precise experimental value for γ_t the masses were determined with an relative error below 1×10^{-5}. Scans with higher resolution show that relative errors of peaks may touch the 10^{-7} range (see fig. 5). Even better precision should be attained by means of operating the ring near transition using a setting with low γ_t.

Compared to typical cooling times for primary beams of less than 1 s, electron cooling of ^{20}Ne fragment beams to equilibrium required between 10 s and 20 s. This time will be reduced hopefully by a factor of 10 after the planned installation of stochastic pre-cooling.

2.4 *Free Electron Target*

The EC beam has been applied also as free electron target with variable energy, W_r, in the center of mass frame of ions. The energy is varied by suitably pulsing the accelerating voltage of the EC device or by applying a pulsed voltage of ± 5 kV to a drift tube in the cooling section. Both methods were combined in a recent experiment on di-electronic recombination processes in order to increase the range for W_r. For this experiment, the desired beam of Li-like Au^{76+} has been breeded from the primarily accumulated beam of He-like Au^{77+}. The rate of recombined Au^{75+}-ions was then measured as a function of W_r by using one of the particle detectors mentioned above [8]. Other experiments using the cooler as free electron target are the investigation of REC by means of X-ray spectra in coincidence with recombined particle detection and the study of laser induced electron capture (LIREC) to high-n states, a process of simultaneous interaction beween photons, electrons and highly charged ions.

3 INTERNAL TARGET EXPERIMENTS

3.1 *Internal Gas Jet*

The internal supersonic gas jet is produced by a Laval nozzle and a four stage differential pumping and skimming system. After crossing the interaction chamber in vertical direction over a free distance of 70 mm, the jet enters a four stage dump [7]. The jet diameter is less than 5 mm, the maximum thickness at the interaction point is presently about 6×10^{12} atoms/cm^2 for Argon and 2×10^{12} atoms/cm^2 for N_2. The maximum UHV-pressure in surrounding chambers is in the low 10^{-9} mbar range and contributes approximately 1% to the total target thickness. It should be noted that the acceptances of the ESR are not affected by the jet target, i. e. there are no aperture limitations in ion beam direction.

Taking into account the numbers of stored ions given in table 1, the presently available luminosity for internal target experiments range from 1×10^{27}cm^{-2}s^{-1} to 2×10^{28}cm^{-2}s^{-1}, depending on ion species and target gas. The design value of 1×10^{30}cm^{-2}s^{-1} is hoped to be attained by improvements of the jet apparatus and by increasing ion beam currents.

3.2 *Beam Target Interaction*

The internal gas jet has been applied to measurements of REC- and stripping cross sections for various ions and for X-ray spectroscopy of H-like ions after REC in the target. It played also an important role for the investigation of a certain mode of nuclear decay (see below). The plot of fig. 5 demonstrates that Schottky spectroscopy is applicable for the analysis of nuclear interactions of electron cooled circulating heavy ions in the jet target. It was recorded after about 400 s interaction of a cooled $^{163}Dy^{66+}$ beam with an Ar-jet and subsequent switching off the jet. The highest (cut) band comes from the primary beam. Several small lines indicate secondary nuclides produced in the jet, which are stored and cooled simultaneously with the primary beam. The larger rightmost peak is explained below. The small $\delta p/p \approx 1.8 \times 10^{-6}$ indicates that, due to the momentum dispersion, the secondary components circulate on orbits, which are well separated from that of the intense primary beam, where they would be heated by IBS.

3.3 *Decay of Stored Nuclei*

There are some stable nuclides getting β^--unstable as soon as the electron cloud has been stripped off. The low Q-value of the decay forbids the emitted electron to escape from the nuclear Coulomb field. The electron is bound to innermost electronic shells. The first experimental proof of this bound-state β^--decay (BBD) took place in 1992 at the ESR [9]. Primary $^{163}Dy^{66+}$ nuclei decayed during long term storage to H-like $^{163}Ho^{66+}$ ions, which have practically the same mass-to-charge ratio as the primary ions and, therefore, circulate on the same orbit as the primary

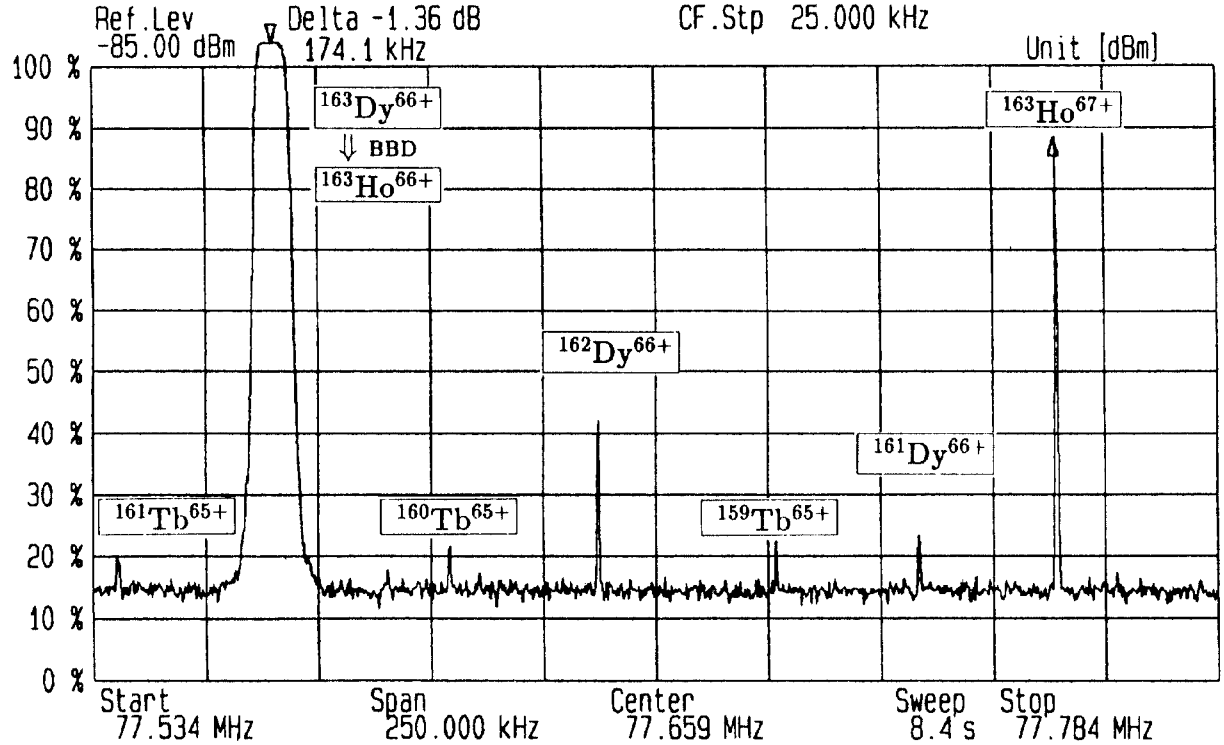

Figure 5: Longitudinal Schottky scan of stored and cooled nuclear fragments produced in ESR at 290 MeV/u in the internal gas jet from primary $^{163}Dy^{66+}$ (large cut band). The peak assigned to $^{163}Ho^{67+}$ — about 20000 out of 2×10^7 primary nuclei — results from bound state β^- decay (see text). Spectra with higher frequency resolution allow precise mass and cross production cross section measurements.

ions. Orbit separation was possible by stripping in the internal gas jet to fully stripped $^{163}Ho^{67+}$ nuclei, which were counted then by a particle detector. Alternatively, after removing the detector out of the aperture, the $^{163}Ho^{67+}$ were stored simultaneously with the primary beam and appeared as a separate band in the Schottky spectrum, which is visible in fig. 5 as the larger rightmost peak. The amount of daughter nuclei — or the peak height in the Schottky scan — normalized to the primary intensity, was measured as a function of storage time. However, the precise determination of the BBD life time τ_{BBD} required complementary measurements of nuclear and atomic cross sections for other charge states and isotopes. The value τ_{BBD}(c.m.)= 50 d $\pm 16\%$ was found by the detector method as well as by Schottky spectroscopy. Similar experiments are envisaged for $^{205}Tl^{81+} \rightarrow {}^{205}Pb^{81+}$ with predicted $\tau_{BBD} \approx 100$ d and $^{187}Re^{75+} \rightarrow {}^{187}Os^{75+}$ with $\tau_{BBD} \approx 10$ y.

4 CONCLUSION AND OUTLOOK

The commissioning of the ESR is by far not complete and will probably never be completed as long as new ideas for experiments are created. But three years of commissioning, operation and internal experiments at the ESR confirm that the ring is a highly versatile instrument. It gives access to new physical systems and novel experimental methods with highest precision and, not least, with comfortable luminosity.

Next steps of more apparative developments are deceleration of fully stripped ions, "ramped" operation of the electron cooler at strongly different energies and installation of a stochastic pre–cooling for hot, radioactive beams. Our interests in beam physics are concentrated on investigations of current and quality limitations of electron cooled bunched and coasting beams, including investigations of impedances and IBS. Further experiments shall deal, e.g., with beam loss by charge changing processes and di electronic recombination for electron rich ions, on line monitoring of the beam target luminosity, and fast bunch compression methods for the production and investigation of hot, dense plasms in solids.

5 REFERENCES

[1] K. Blasche et al., these proceedings

[2] H. Eickhoff et al., these proceedings

[3] H. Geissel et al., Nucl. Instr. and Meth. **A282**, 247 (1989)

[4] B. Franzke, Nucl. Instr. and Meth. **B24/25**, 18 (1987)

[5] M. Steck et al., these proceedings

[6] N. Angert et al., *Proc. of Europ. Part. Accel. Conf., Rome, 1988*, World Scientific (1989) p. 1436

[7] A. Gruber et al., Nucl. Instr. and Meth. **A282**, 87 (1989)

[8] W. Spies et al., Phys. Rev. Letters **69**, No. 19, 2768 (1992)

[9] M. Jung et al., Nucl. Physics **A553**, 309c (1993)